Heat Transfer—Asian Research, **36** (7), 2007

A Study on Membrane Distillation by a Solar Thermal-Driven System

Tsung-Ching Chen, Chii-Dong Ho, Jia-Jan Guo, and Jr-Wei Tu
Department of Chemical and Materials Engineering, Tamkang University,
Tamsui, Taiwan 251, R.O.C.

Membrane distillation (MD) is a membrane separation process that has long been investigated in small scale laboratory studies and has the potential to become a viable tool for water desalination. MD is a separation process that combines simultaneous mass and heat transfer through a hydrophobic microporous membrane. A solar collector is used in direct contact membrane distillation (DCMD) to heat seawater as a temperature driving force in heat transfer to establish seawater desalting systems. The effect of the temperature difference makes the brine vaporize in the hot fluid side and condense in the cold fluid side. The optimal operating parameters on the pure water production rate will also be examined in this study. The purposes of this study are to develop the theoretical heat and mass transfer formulations, simulate heat transfer rate of solar collector with internal fins in membrane distillation, and investigate the mass-transfer efficiency improvement in membrane distillation with the brine flow rate, solar collector efficiency, and temperature difference between both sides of membrane as parameters. © 2007 Wiley Periodicals, Inc. Heat Trans Asian Res, 36(7): 417–428, 2007; Published online in Wiley InterScience (www.interscience.wiley.com). DOI 10.1002/htj.20172

Key words: membrane distillation, solar collector, seawater desalination, pure water productivity

1. Introduction

Membrane distillation (MD) is an innovative membrane separation process to extract pure water from seawater, brackish water, or waste water. The pure water in vapor form transports through a hydrophobic membrane while a temperature gradient is established across the membrane resulting in a vapor pressure difference as a driving force. The benefits of MD as compared to the convectional processes to produce pure water, say distillation or reverse osmosis (RO), are: (1) lower operating temperature than distillation, (2) lower operating pressure than RO, (3) lower energy requirement, (4) smaller module size, and (5) higher purity of the produced water [1]. There are four categories of MD: direct contact membrane distillation (DCMD) [2–4], air gap membrane distillation (AGMD) [5, 6],

Contract grant sponsor: National Science Council of the Republic of China; grant number: NSC 94-2212-E-032-014

vacuum membrane distillation (VMD) [7, 8], and sweeping gas membrane distillation (SGMD) [9–11]. The DCMD is the simplest type to operate and it is also best suited to desalt or concentrate aqueous solutions while the water is the major permeate component. In the DCMD, the hydrophobic membrane directly contacts the liquid phases on both sides. The water initially vaporizes in the liquid phase under the higher temperature, then transports through the pores of the hydrophobic membrane and condenses immediately in the cold liquid phase. In general, the mass transfer rate of water vapor through the membrane can be improved by changing the properties of the hydrophobic membrane [12, 13], enhancing the turbulence of fluid on the membrane surface [14], increasing the fluid flow rate and the inlet temperature difference [15], and changing the conduit geometries [16].

The heat source used in the type of DCMD of this study is afforded by a sheet-and-tube solar water heater with fins attached, which is referred to as solar thermal-driven membrane distillation. The sheet-and-tube solar water heater consists of one glass sheet above an absorbing plate and the fluid flowing in the metallic tubes under the absorbing plate. The sheet-and-tube solar water heater is a kind of flat-plate solar collector and is mechanically simpler than the concentrating solar collector. The blackened absorber absorbs the solar radiant energy and transforms it to thermal energy, and thus the fluid, say seawater, in the metallic tubes receives the heat from the absorber via the heat conduction of the metallic tubes. The heated seawater exits from the sheet-and-tube solar water heater and then feeds into the DCMD module as the hot liquid phase while the cold liquid phase is the pure water pumped from the storage tank. Moreover, the strategies of improving a flat-plate solar collector performance involves: (1) extending the heat transfer area [17], (2) enhancing the fluid turbulence [18, 19], (3) strengthening the free convection of fluid [20], (4) reducing heat loss by using the glass covers above the absorber [21], (5) adjusting the aspect ratio of the collector, (6) regulating the fluid inlet temperature, flow rate [22], and (7) adding the external recycle to enhance the force heat convection of fluid [23, 24].

The purposes of this work are to develop a two-dimensional mathematical formulation for the solar thermal-driven DCMD module, investigate the effects of feed flow rate and inlet temperature gradient on the temperature distribution of fluid and pure water productivity, and calculate the required collector area of the sheet-and-tube solar water heater to provide sufficient thermal energy for the DCMD process.

Nomenclature

A_c: surface area of the collector (m^2)
a_{water}: activity of water in NaCl solution
B_m: the horizontal width of membrane distillation apparatus (m)
C_b: conductance of bond (kJ/(s·m·K))
C_m: membrane coefficient (kg/(s·m^2·Pa))
C_P: specific heat of water at constant pressure (kJ/(kg·K))
D: outside diameter of tube (m)
D_h: equivalent hydraulic diameter of tubes with/without fins attached (m)
D_i: inside diameter of tube (m)
d_i: height of channel i (m)
F: sheet standard efficiency
F'_{fin}: collector efficiency factor of solar collector with fins attached

f_F: Fanning friction factor
H_{fin}: height of internal fins (m)
H_R: hydraulic dissipate energy with recycle operation and fins attached (hp)
$h_{f,i}$: convective heat-transfer coefficient inside tube (kJ/(s·m^2·K))
I_0: incident solar radiation (kJ/(s·m^2))
k_{fa}: thermal conductivity of fluid *a* (kJ/(s·m·K))
k_{fb}: thermal conductivity of fluid *b* (kJ/(s·m·K))
k_m: thermal conductivity of membrane (kJ/(s·m·K))
L: total length of membrane distillation device (m)
L_s: total length of tubes (m)
M: mass flow rate of solar water heater (kg/min)
m: total water mass flow rate of solar water heater (kg/min)
m_{flux}: total mass of pure water transfer across membrane (kg/s)
N: pure water flux (kg/(s·m^2))
N_f: number of fins attached
n: number of pair ducts
P_i: partial vapor pressure of component *i* (Pa)
P_i^0: saturated vapor pressure of component *i* (Pa)
Q_u: total useful gain of solar water heater (kJ/s)
q_u': useful energy of solar water heater with fins attached (kJ/(s·m))
S: useful energy of absorbing plate from the sun (kJ/(s·m^2))
T_a: ambient temperature (K)
$T_a(x_a, z)$: temperature distribution of channel *a* (K)
T_{hotin}: inlet fluid temperature of NaCl solution (K)
$T_b(x_b, z)$: temperature distribution of channel *b* (K)
T_{coldin}: inlet fluid temperature of water (K)
$T_{f,0}$: inlet temperature of water of solar water heater (K)
$T_{f,\text{out}}$: outlet temperature of water of solar water heater (K)
$T_f(z)$: temperature distribution of fluid of solar water heater (K)
U_L: overall loss coefficient (kJ/(s·m^2·K))
V_i: volumetric flow rate of channel *i* (m^3/s)
v: fluid velocity of solar water heater (m/s)
$\overline{v}_i$: mean velocity of channel *i* (m/s)
$v_i(x_i)$: velocity profile of channel *i* (m/s)
W: distance between tubes (m)
x_i: mole fraction of component *i*
α_{mi}: thermal diffusivity of component *i* (m^2/s)
δ_m: thickness of membrane (m)
η_e: collector efficiency
η_f: fin efficiency
λ: latent heat of water (kJ/kg)
ρ_{mi}: density of component *i* (kg/m^3)

2. Thermal Efficiencies of Sheet-and-Tube Solar Water Heater with Fins Attached

The sheet-and-tube solar water heater with fins attached plays the role of thermal supply for membrane distillation process. Its schematic diagram is shown in Fig. 1. The main simplified assumptions and approximations in the calculation procedure are as follows: (1) the inlet concentration of NaCl solutions is time-independent; (2) the physical properties are constants in each theoretical prediction; (3) the effect of concentration polarization on membrane surface is neglected. The useful energy gain per unit length in the flow direction from the blackened absorber by fluid was obtained as

$$q_u' = WF_{fin}'[S - U_L(T_f(z) - T_a)] \tag{1}$$

where the collector efficiency factor with fins attached F_{fin}' is

$$F_{fin}' = \left\{ WU_L \left[\frac{1}{U_L[(W-D)F+D]} + \left[\frac{1}{(h_{f,i}\pi D_i)} + \frac{1}{C_b} \right] \left(1 - \frac{2N_f \eta_f h_{f,i} H_{fin}}{U_L[(W-D)F+D]} \right) \right] \right\}^{-1} \tag{2}$$

After making the energy balance in a fluid element, one may derive the following equations for calculating the outlet fluid temperature of the sheet-and-tube solar water heater

$$M_1 C_p \frac{dT_{f,1}(z)}{dz} - WF_{fin}'[S - U_L(T_{f,1}(z) - T_a)] = 0 \tag{3}$$

$$-M_2 C_p \frac{dT_{f,2}(z)}{dz} - WF_{fin}'[S - U_L(T_{f,2}(z) - T_a)] = 0 \tag{4}$$

where the mass flow rate in each tube is $M_1 = M_2 = m(R+1)/n$. The performance of the solar water heater can be obtained by defining the collector efficiency η_e

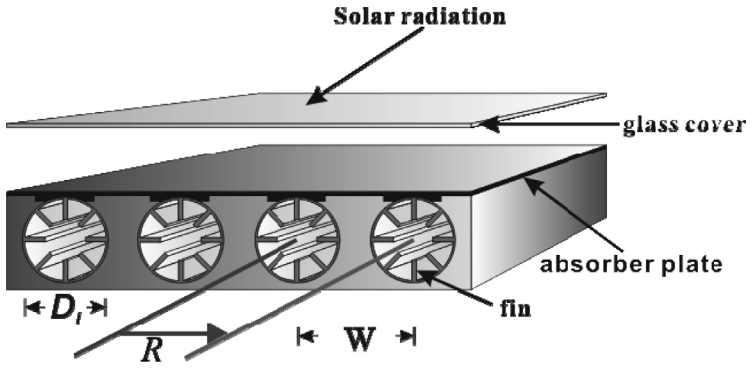

Fig. 1. Sheet-and-tube solar water heater with fins attached.

$$\eta_e = Q_u/A_cI_0 = mC_p(T_{f,\text{out}} - T_{f,0})/A_cI_0 \tag{5}$$

The hydraulic dissipate energy of the double-pass device with recycle operation and fins attached can be estimated as

$$H_R = (M_1 + M_2)(2f_F v^2 L_s/D_h) \tag{6}$$

3. Temperature Distributions in Direct Contact Membrane Distillation Module

Figure 2 shows a parallel-flow membrane distillation device. The open conduit is divided into two parts, channel *a* and channel *b*, by inserting a hydrophobic membrane in it. The equations of heat transfer and velocity distributions are as follows:

$$k_{fa}\frac{\partial^2 T_a(x_a, z)}{\partial x_a^2} = \rho_{ma}C_{p,a}v_a(x_a)\frac{\partial T_a(x_a, z)}{\partial z} \tag{7}$$

$$k_{fb}\frac{\partial^2 T_b(x_b, z)}{\partial x_b^2} = \rho_{mb}C_{p,b}v_b(x_b)\frac{\partial T_b(x_b, z)}{\partial z} \tag{8}$$

$$v_i(x_i) = 6\overline{v_i}(x_i/d_i - x_i^2/d_i^2),\ (i = a, b) \tag{9}$$

The boundary conditions for solving Eqs. (7) and (8) are

$$T_a(x_a, 0) = T_{\text{hotin}} \tag{10}$$

$$k_{fa}\frac{\partial T_a(d_a, z)}{\partial x_a} = -(N\lambda + k_m(T_a(d_a, z) - T_b(d_b, z))/\delta_m) \tag{11}$$

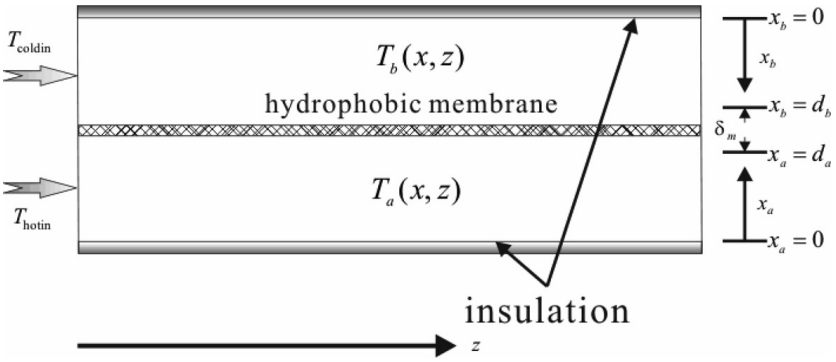

Fig. 2. Parallel-flow diagram of membrane distillation apparatus.

$$\frac{dT_a(0,z)}{dx_a}=0 \tag{12}$$

$$T_b(x_b,0)=T_{\text{coldin}} \tag{13}$$

$$k_{fb}\frac{\partial T_b(d,z)}{\partial x}=N\lambda+k_m(T_a(d_a,z)-T_b(d_b,z))/\delta_m \tag{14}$$

$$\frac{dT_b(0,z)}{dx_b}=0 \tag{15}$$

By introducing a general technique, method of lines, for solving Eqs. (7) and (8), the partial differential equations can be reduced to ordinary differential equations via finite difference relationships. The equations of heat transfer in Eqs. (7) and (8) can be rewritten by the following form

channel *a*

$$\frac{\partial T_{a1}(x_{a1},z)}{\partial z}=\frac{\alpha_{ma}}{v_a(x_{a1})}\left(\frac{T_{a2}-2T_{a1}+T_{a0}}{\Delta x_a^2}\right) \tag{16}$$

$$\frac{\partial T_{a2}(x_{a2},z)}{\partial z}=\frac{\alpha_{ma}}{v_a(x_{a2})}\left(\frac{T_{a3}-2T_{a2}+T_{a1}}{\Delta x_a^2}\right) \tag{17}$$

$$\vdots$$

$$\frac{\partial T_{an}(x_{an},z)}{\partial z}=\frac{\alpha_{ma}}{v_a(x_{an})}\left(\frac{T_{a(n+1)}-2T_{an}+T_{a(n-1)}}{\Delta x_a^2}\right) \tag{18}$$

channel *b*

$$\frac{\partial T_{b1}(x_{b1},z)}{\partial z}=\frac{\alpha_{mb}}{v_b(x_{b1})}\left(\frac{T_{b2}-2T_{b1}+T_{b0}}{\Delta x_b^2}\right) \tag{19}$$

$$\frac{\partial T_{b2}(x_{b2},z)}{\partial z}=\frac{\alpha_{mb}}{v_b(x_{b2})}\left(\frac{T_{b3}-2T_{b2}+T_{b1}}{\Delta x_b^2}\right) \tag{20}$$

$$\vdots$$

$$\frac{\partial T_{bn}(x_{bn},z)}{\partial z}=\frac{\alpha_{mb}}{v_b(x_{bn})}\left(\frac{T_{b(n+1)}-2T_{bn}+T_{b(n-1)}}{\Delta x_b^2}\right) \tag{21}$$

and the reduced boundary conditions are

channel *a*

$$T_{an}|_{z=0} = T_{\text{hotin}},\ n = 1, 2, 3\ldots \tag{22}$$

$$T_{a(n+1)} = (4T_{an} - T_{a(n-1)} - 2\Delta x_a(N\lambda + k_m(T_{an} - T_{bn})/\delta_m)/k_{fa})/3 \tag{23}$$

$$T_{a0} = (4T_{a1} - T_{a2})/3 \tag{24}$$

channel *b*

$$T_{bn}|_{z=0} = T_{\text{coldin}},\ n = 1, 2, 3\ldots \tag{25}$$

$$T_{b(n+1)} = (4T_{bn} - T_{b(n-1)} - 2\Delta x_b(N\lambda + k_m(T_{an} - T_{bn})/\delta_m)/k_{fb})/3 \tag{26}$$

$$T_{b0} = (4T_{b1} - T_{b2})/3 \tag{27}$$

The total mass of pure water transfer across membrane can be determined by

$$\frac{dm_{flux}}{dz} = NB_m \tag{28}$$

The pure water flux N is a function of vapor pressure drop across the membrane

$$N = C_m\Delta P = C_m(P_{m,a} - P_{m,b}) \tag{29}$$

where C_m is the membrane coefficient. For non-idea binary mixtures, the partial pressures can be determined from

$$P_i = y_iP = x_ia_iP_i^0 \tag{30}$$

The activity of water in NaCl solutions can be determined by [1]

$$a_{water} = 1 - 0.5x_{\text{NaCl}} - 10x_{\text{NaCl}}^2 \tag{31}$$

The vapor pressure of water is determined by Antoine equation as follows:

$$P_i^0 = \exp(23.238 - 3841/(T - 45)) \tag{32}$$

Substituting Eqs. (30)–(32) into Eq. (29), one may obtain the following relations

$$N = C_m\left(x_{water}a_{water}\exp\left(23.238 - \frac{3841}{T_{a(n+1)} - 45}\right) - \exp\left(23.238 - \frac{3841}{T_{b(n+1)} - 45}\right)\right) \tag{33}$$

Substituting the boundary conditions into Eqs. (16)–(21), the system of ordinary differential equations with initial boundary conditions as well as Eq. (28) was solved simultaneously by using the fourth-order Runge–Kutta method and the theoretical production of pure water is thus obtained.

4. Results and Discussion

The working dimensions of the present solar thermal-driven direct contact membrane distillation device are as follows: conduit length L = 0.2 m, channel height H = 0.002 m, and width B = 0.15 m. The membrane coefficient of hydrophobic membrane referred to experimental results of Schofield et al. [25] is $C_m = 4.5 \times 10^7$ kg/(s·m^2·Pa). The pure water flux can be determined by Eq. (33) and the calculated results are shown in Fig. 3 with the inlet cold water temperature as a parameter under the given working dimensions. The theoretical results show that the pure water flux increases with increasing the inlet hot NaCl temperature T_{hotin} but decreases with increasing the inlet cold water temperature T_{coldin}. This transport phenomenon can be attributed to whether the temperature gradient between cold and hot fluid increases by increasing T_{hotin} or decreasing T_{coldin}, and thus the vapor pressure difference increases to lead to enhancing the mass transfer rate of the pure water. Meanwhile, the temperature polarization phenomenon on the membrane is an important factor of hindering the pure water flux in a DCMD process due to the heat conduction and water vaporization across the membrane. The undesired effect can be overcome by increasing the volumetric flow rate of fluid, resulting in the heat convection coefficient improvement which is proportional to volumetric flow rate of fluid. The pure water flux increases with increasing the volumetric flow rate of fluid in the channels *a* or *b* as confirmed in Fig. 4. Figure 5 shows the temperature distribution on both membrane surfaces in the flowing direction (z). The membrane surface temperature of hot side $T_a(d_a, z)$ decreases along with z while the membrane surface temperature of cold side $T_b(d_b, z)$ rises with increasing z as indicated in Fig. 5. Moreover, the difference between the two temperatures $T_a(d_a, z)$ and $T_b(d_b, z)$ in Fig. 5 decreases along the flow direction, but the temperature difference decrement versus z is limited as the DCMD processes take place. The temperature gradient on the membrane is the main mass-

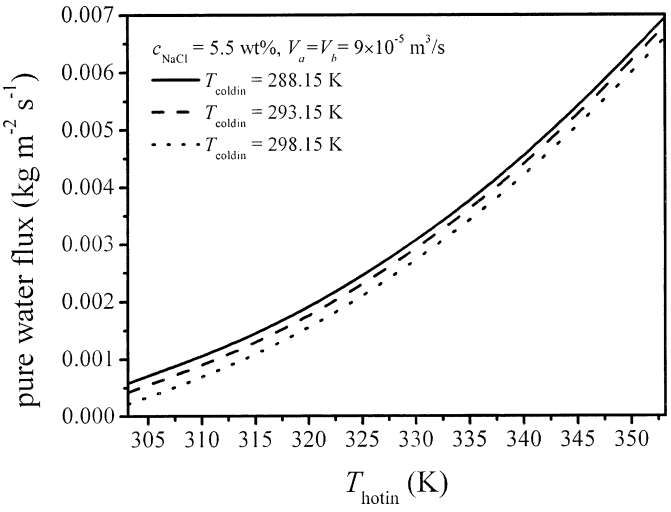

Fig. 3. Effect of fluid temperature on pure water flux.

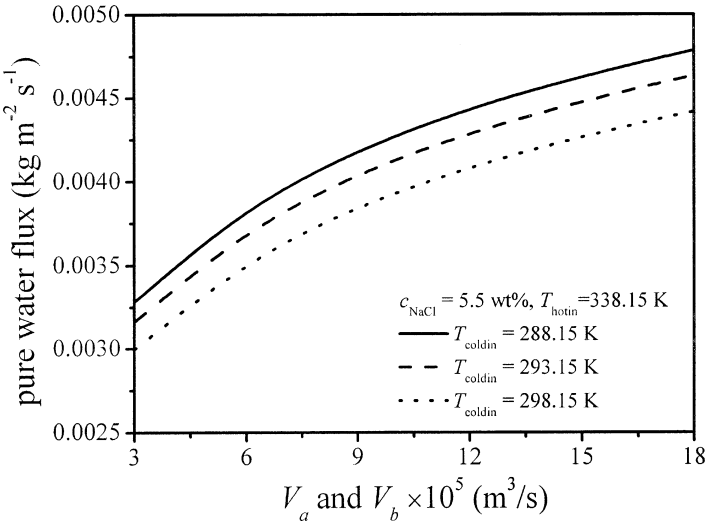

Fig. 4. Effect of fluid velocities of both channels on pure water flux.

transfer driving force in the DCMD and the higher temperature gradient leads to the higher pure water flux as concluded from Fig. 3. Therefore, it is seen that the pure water flux decreases with flowing direction due to the temperature difference decreasing along the flowing direction as shown in Fig. 5. Although increasing the membrane area with a fixed horizontal width of channel has the advantage on total productivity of pure water, the pure water flux decreases with increasing the length of channel. There exists an optimal adjustment on the membrane distillation parameters to make good economic sense (i.e., the initial cost of membrane and operating cost).

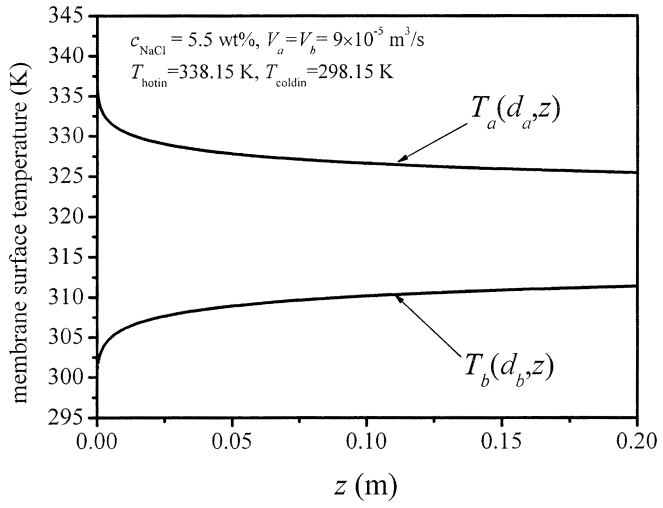

Fig. 5. Temperature distribution on the membrane surface along z-axis.

Before entering the membrane distillation module, a sheet-and-tube solar water heater is used to preheat the NaCl solution to establish a temperature difference with the cold water feed in this study. The scheme of the sheet-and-tube solar water heater is shown in Fig. 1. The recycle-operation device with fins attached on the sheet-and-tube solar water heater can enhance the heat transfer rate to reduce the required collector area for preheating the NaCl solution and these advantage designs have been reported in the previous works [19, 24]. For the case of both temperatures T_{hotin} and T_{coldin} are 338.15 K and 298.15 K, respectively, in the MD module as shown in Fig. 5, the outlet fluid temperature of the hot NaCl solution is estimated to 336.78 K under steady-state operation. Hence, the required collector area of the sheet-and-tube solar water heater operation to preheat the NaCl solution from 336.78 K to 338.15 K is calculated by the following working dimensions and operating conditions of the sheet-and-tube solar water heater: distance between two tubes = 0.2 m, number of pair ducts = 5, number of fins attached = 2, mass flow rate of NaCl solution = 0.093 kg/s, recycle ratio = 1, and incident solar radiation = 1.0 kJ/(m^2·s). The calculated result of the required collector area is of 1.1 m^2 and the corresponding collector efficiency calculated by Eq. (5), and the hydraulic dissipate energy calculated by Eq. (6), are 0.487 and 7.32×10^{-4} hp, respectively.

5. Conclusion

The mathematical model of the direct contact membrane distillation (DCMD) coupled with the sheet-and-tube solar water heater has been developed theoretically in this study. The theoretical prediction of the pure water flux is obtained by the energy balance equations with the use of the fourth-order Runge–Kutta method. The influences of the inlet fluid temperature and volumetric flow rate of both hot NaCl solution and cold water on the pure water flux are shown in Figs. 3–5. The calculated results can be summarized as follows: (1) the production of pure water increases with increasing the hot NaCl temperature but with decreasing the cold water temperature; (2) the production of pure water increases with increasing the volumetric flow rate of the hot NaCl solution and the volumetric flow rate of the cold water due to the minimization of the temperature polarization phenomenon on the membrane surface; (3) the pure water flux decreases along with the flowing direction; (4) the required collector area for preheating the hot NaCl solution from 336.78 K to 338.15 K is about 1.1 m^2 in the present study.

It may be stated from the above results that the possibility of incorporating solar heating technology into membrane distillation device to reduce additional energy cost for preheating the NaCl solution and thus the greenhouse effect is reduced. A further study will be conducted on the experimental run of DCMD membrane distillation to confirm the theoretical formulation. The theoretical perdition of this study is useful to explain the temperature polarization phenomena on membrane surface of DCMC membrane distillation. This is the value of the present study.

Acknowledgment

The authors thank the National Science Council of the Republic of China for its financial support.

Literature Cited

1. Kevin WL, Douglas RL. Membrane distillation. J Mem Sci 1997;124:1–25.

2. Fujii Y, Kigoshi S, Iwatani H, Aoyama M. Selectivity and characteristics of direct contact membrane distillation type experiment. I. Permeability and selectivity through dried hydrophobic fine porous membranes. J Mem Sci 1992;72:53–72.
3. Fujii Y, Kigoshi S, Iwatani H, Aoyama M, Fusaoka Y. Selectivity and characteristics of direct contact membrane distillation type experiment. II. Membrane treatment and selectivity increases. J Mem Sci 1992;72:73–89.
4. Ding Z, Ma R, Fane AG. A new model for mass transfer in direct contact membrane distillation. Desalination 2002;147:133–138.
5. Izquierdo-Gil MA, Garcia-Payo MC, Fernandez-Pineda C. Air gap membrane distillation of sucrose aqueous solutions. J Mem Sci 1998;144:45–56.
6. Garcia-Payo MC, Izquierdo-Gil MA, Fernandez-Pineda C. Air gap membrane distillation of aqueous alcohol solutions. J Mem Sci 2000;169:61–80.
7. Bandini S, Gostoli C, Sarti GC. Separation efficiency in vacuum membrane distillation. J Mem Sci 1992;73:217–229.
8. Sarti GC, Gostoli C, Bandini S. Extraction of organic components from aqueous streams by vacuum membrane distillation. J Mem Sci 1993;80:21–33.
9. Basini L, D'Angelo G, Gobbi M, Sarti GC, Gostoli C. A desalination process through sweeping gas membrane distillation. J Mem Sci 1987;64:245–257.
10. Rivier CA, Garcia-Payo MC, Marison IW, Stocker UV. Separation of binary mixtures by thermostatic sweeping gas membrane distillation I. Theory and simulations. J Mem Sci 2002;201:1–16.
11. Rivier CA, Garcia-Payo MC, Marison IW, von Stocker U. Separation of binary mixtures by thermostatic sweeping gas membrane distillation II. Experimental results with aqueous formic acid solutions. J Mem Sci 2002;198:197–210.
12. Phattaranawik J, Jiraratananon R, Fane AG. Effect of pore size distribution and air flux on mass transport in direct contact membrane distillation. J Mem Sci 2003;215:75–87.
13. Martinez L, Florido-Diaz FJ, Hernandez A, Pradanos P. Characterisation of three hydrophobic porous membranes used in membrane distillation modelling and evaluation of their water vapour permeabilities. J Mem Sci 2002;203:15–27.
14. Phattaranawik J, Jiraratananon R, Fane AG, Halim C. Mass flux enhancement using spacer filled channels in direct contact membrane distillation. J Mem Sci 2001;187:193–201.
15. Phattaranawik J, Jiraratananon R, Fane AG. Heat transport and membrane distillation coefficients in direct contact membrane distillation. J Mem Sci 2003;212:177–193.
16. Koschikowski J, Wieghaus M, Rommel M. Solar thermal-driven desalination plants based on membrane distillation. Desalination 2003;156:295–304.
17. Seluck MK. Solar air heaters and their applications. Academic Press; 1977.
18. Yeh HM, Ting YC. Efficiency of solar air heaters packed with iron filings. Energy 1988;13:543–547.
19. Yeh HM, Ho CD, Hou JZ. Collector efficiency of double-flow solar air heaters with fins attached. Energy 2002;27:715–727.
20. Kreith F, Kreider JF. Principles of solar engineering. McGraw-Hill; 1978.
21. Yeh HM, Ho CD, Hou JZ. Collector efficiency of double-flow baffled solar air heaters. J Chin Inst Chem Engrs 2000;31:617–622.
22. Yeh HM, Ho CD, Lin CY. Effect of collector aspect ratio on the collector efficiency of upward type baffled solar air heaters. Energy Convers Manage 2000;41:971–981.
23. Ho CD, Yeh CW, Hsieh SM. Improvement in device performance of multi-pass flat-plate solar air heaters with external recycle. Renewable Energy 2006;30:1601–1621.
24. Ho CD, Chen TC. The recycle effect on the collector efficiency improvement of double-pass sheet-and-tube solar water heaters with external recycle. Renewable Energy 2006;31:953–970.

25. Schofield RW, Fane AG, Fell CJD. Heat and mass transfer in membrane distillation. J Mem Sci 1987;33:299–313.

□♦ ♦ ♦□

Originally published in 2006 Symposium of Transport Phenomena and Applications, Taipei, Sept. 29, 2006, pp. 1–4.

Translated by Tsung-Ching Chen, Chii-Dong Ho, Jia-Jan Guo, and Jr-Wei Tu, Department of Chemical and Materials Engineering, Tamkang University, Tamsui, Taiwan 251, R.O.C.